Available online at www.sciencedirect.com
SCIENCE DIRECT®
Chemical Physics Letters 372 (2003) 569–576
CHEMICAL PHYSICS LETTERS
www.elsevier.com/locate/cplett

Reactions of HOBr + HCl + nH$_2$O and HOBr + HBr + nH$_2$O

Andreas F. Voegele [a,*], Christofer S. Tautermann [a], Thomas Loerting [b], Klaus R. Liedl [a,*]

[a] Department of Theoretical Chemistry, University of Innsbruck, Innrain 52a, A-6020 Innsbruck, Austria
[b] Department of Earth, Atmosphere and Planetary Sciences, Massachusetts Institute of Technology, 77 Massachusetts Avenue, Cambridge, MA 02139-4307, USA

Received 31 January 2003; in final form 11 March 2003

Abstract

The reactions of HOBr with HCl and HBr in the presence of $n = 0$, 1, 2 and 3 water molecules are investigated by hybrid density functional theory methods in combination with canonical, variational transition state theory including tunneling corrections. Compared to the reactions of HOCl with HCl and HBr [J. Phys. Chem. A 106 (2002) 7850], we found that the barriers of the title reactions are significantly lower yielding much higher rate constants. Support of only two water molecules makes the reaction of HOBr with HBr barrierless. Under stratospheric conditions the reactions of HOBr with HBr are the most reactive ones.

1. Introduction

Heterogeneous reactions on the surfaces of polar stratospheric clouds (PSCs) play a key role in the seasonally recurring ozone depletion observed in the stratosphere of Antarctica. Particularly, reactions of the so-called halogen reservoir species such as ClONO$_2$, HCl, BrONO$_2$ and HBr on PSCs are of great importance. These heterogeneous reactions lead to reactivation of the stored inactive halogen atoms, which are in turn responsible for ozone depletion [1,2]. The first step of activation of these reservoir species mostly involves hydrolysis of chlorine and bromine nitrate [3,4]

$$\mathrm{ClONO_2 + H_2O \rightleftarrows HOCl + HNO_3} \quad (1)$$

$$\mathrm{BrONO_2 + H_2O \rightleftarrows HOBr + HNO_3} \quad (2)$$

In the next step the reaction products of reactions (1) and (2), HOCl and HOBr, are activated by two different mechanisms yielding more reactive species, that participate directly in the ozone depletion cycle. Either, these molecules are photolyzed in the presence of sunlight, or they react with the hydrogen halides HCl and HBr heterogeneously [5,6]. Reactions of HOCl have been well investigated both experimentally [5,6] and theoretically [7–10]. In an accompanying study [11] we have investigated the reactions of HOCl with the hydrogen halides in model water clusters. In the

* Corresponding authors. Fax: +43-512-507-5144 (K.R. Liedl).
E-mail addresses: andreas.voegele@uibk.ac.at (A.F. Voegele), klaus.liedl@uibk.ac.at (K.R. Liedl).

0009-2614/03/$ - see front matter
doi:10.1016/S0009-2614(03)00447-0

present study we concentrate on the reactions of HOBr with HCl and HBr

$$HOBr + HCl \rightleftarrows BrCl + H_2O \quad (3)$$

$$HOBr + HBr \rightleftarrows Br_2 + H_2O \quad (4)$$

Reactions of bromine species are of special importance for stratosphere and the ozone layer, since the ozone depletion potential of bromine is estimated to be up to two orders of magnitude higher than the ozone depletion potential of chlorine [2,12]. Recent studies have therefore investigated the effect of bromine species on the ozone concentration [13,14]. Since reactions (3) and (4) are key reactions for bromine activation, heterogeneous reactions of HOBr have been investigated experimentally [15,16]. Yet, up to now there are no theoretical studies on the reactions of HOBr with HCl or HBr, except for characterization of halogen anion–HOBr complexes [17]. In this study we present detailed mechanisms and reaction rate constants for reactions (3) and (4) in model water clusters of different size. These water clusters are a simple model to mimick heterogeneous ice surfaces as present in PSCs of type II. We compare our results with a previous study on the reaction of HOCl with HCl and with HBr in model water clusters [11].

2. Methods

In order to compare the title reactions with our previous study, where we investigated the reactions of HOCl with HCl and HBr, we used the same methods as described before [11]. Thus, in the following section we will only briefly summarize the used methods.

Stationary points were determined with hybrid density functional theory (DFT) at different levels of theory – B3LYP/6-31+G(d), B3LYP/6-311++G(d,p) [18], and MPW1K/6-31+G(d,p) [19] – using the GAUSSIAN 98 program package [20]. Vibrational analysis confirmed the nature of the stationary points.

The reaction path connecting the minima was created as the minimum energy path (MEP) starting from the transition state in mass scaled coordinates (scaling mass 1 amu). The Page–McIver local quadratic approximation algorithm [21] and B3LYP/6-31+G(d) were used at a step size of 0.050 bohr. Distances on the potential energy surface (PES) from the transition state are denoted by s, with s being positive on the product side and negative on the educt side. Every third point second derivatives were determined. Since the B3LYP method normally underestimates reaction barriers [22], we interpolated the PES to energy values determined by MPW1K/6-31+G(d,p). MPW1K was optimized on a set of experimental reaction barriers and is designed to calculate reaction rate constants. The interpolation procedure is based on a logarithmic procedure [23] and will be termed MPW1K/6-31+G(d,p)///B3LYP/6-31+G(d).

Reaction rates were obtained using variational transition state theory (VTST) as implemented in Polyrate9.0 [24,25]. A brief outline of the concepts of VTST is given below, yet for details we refer to other papers [26–30]. A microcanonical ensemble was used to obtain a rate constant k minimized with respect to barrier crossings of a classical flux of particles on the PES. Quantum mechanical effects along the reaction coordinate are treated by semi-classical theory to evaluate transmission probabilities. Inclusion of these quantum mechanical effects on the reaction rate constant is carried out by multiplying k by a ground state transmission coefficient κ. The methods we consider for determining κ are the small curvature tunneling (SCT) and the large curvature tunneling (LCT) approach. SCT is considered by means of the centrifugal dominant small curvature semiclassical adiabatic ground state tunneling method [31]. For LCT we employed the large curvature ground state approximation version 4 (LCG4) [32]. The maximum of the SCT and LCT transmission coefficients was used for the tunneling correction according to the microcanonical optimized multidimensional tunneling (μOMT) approach.

3. Results and discussion

3.1. Stationary points, energetics, and reaction mechanisms

We characterized stationary structures for the reactions of HOBr with HCl in the presence of

$n = 0$, 1, 2 and 3 water molecules (see Fig. 1 for schematic representation of the reactions and Fig. 2 for the structures of the transition states). Compared to the reactions HOCl + HCl + nH$_2$O ($n = 0$, 1, 2 and 3), there are only little differences in the stationary structures except for slightly altered bond lengths as a result of substitution of Cl by Br. Mostly, the reaction barriers determined at the B3LYP levels of theory are smaller than those at the MPW1K/6-31+G(d,p) level. This is in accordance with our previous findings [11] and is what we should expect since MPW1K was designed for determining barriers, whereas B3LYP is known to underestimate reaction barriers [22] (see Table 1). If not indicated otherwise, the barriers in the text refer to MPW1K/6-31+G(d,p) values. The values determined with B3LYP/6-31+G(d) are very close to that ones determined with B3LYP/6-311++G(d,p), justifying calculation of the PES at the lower level of theory.

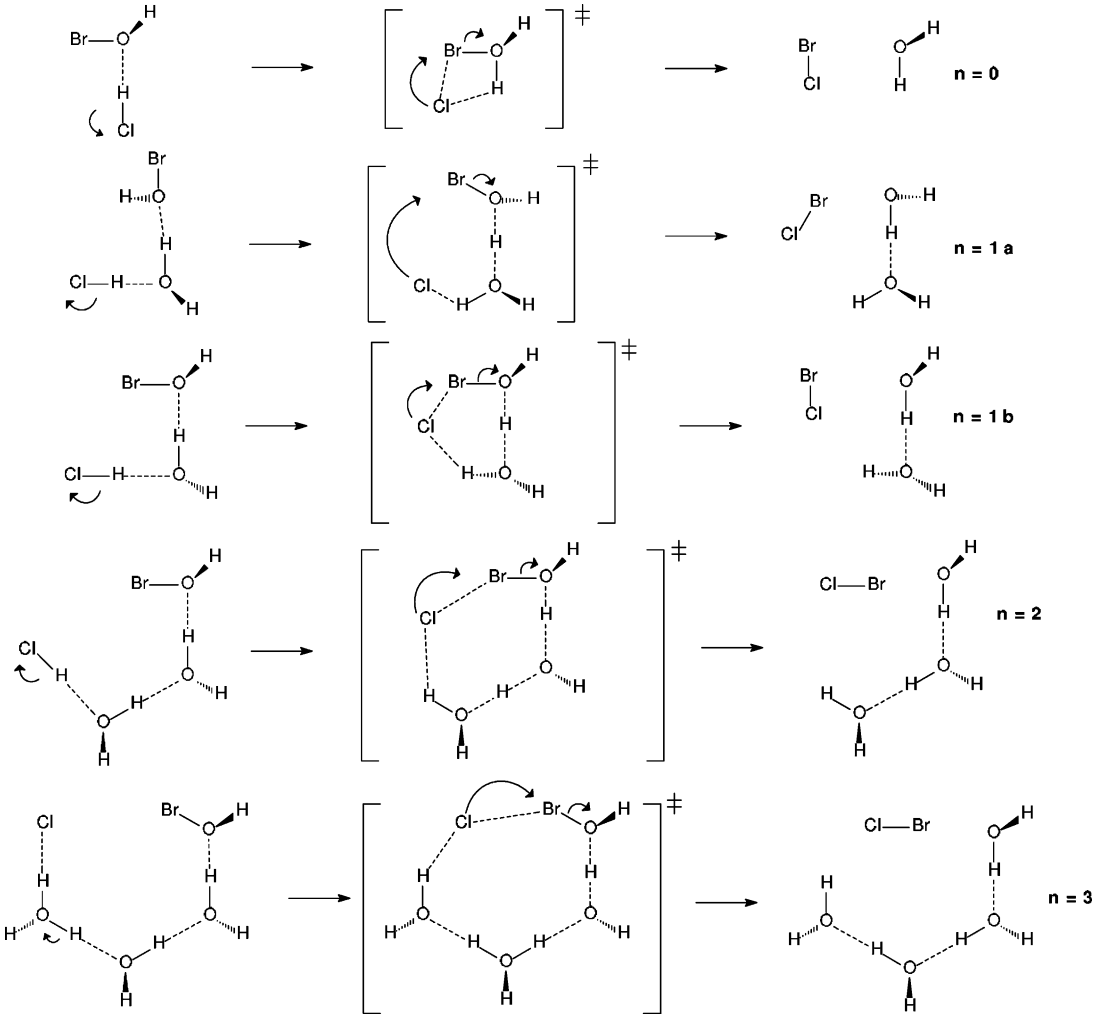

Fig. 1. Qualitative representation of the stationary points of the reaction of HOBr + HCl supported by $n = 0$, 1, 2 and 3 water molecules. The reactions of HOBr + HBr with $n = 0$ and 1 water molecules yield analogous structures, whereas for $n \geqslant 2$ no transition states could be found.

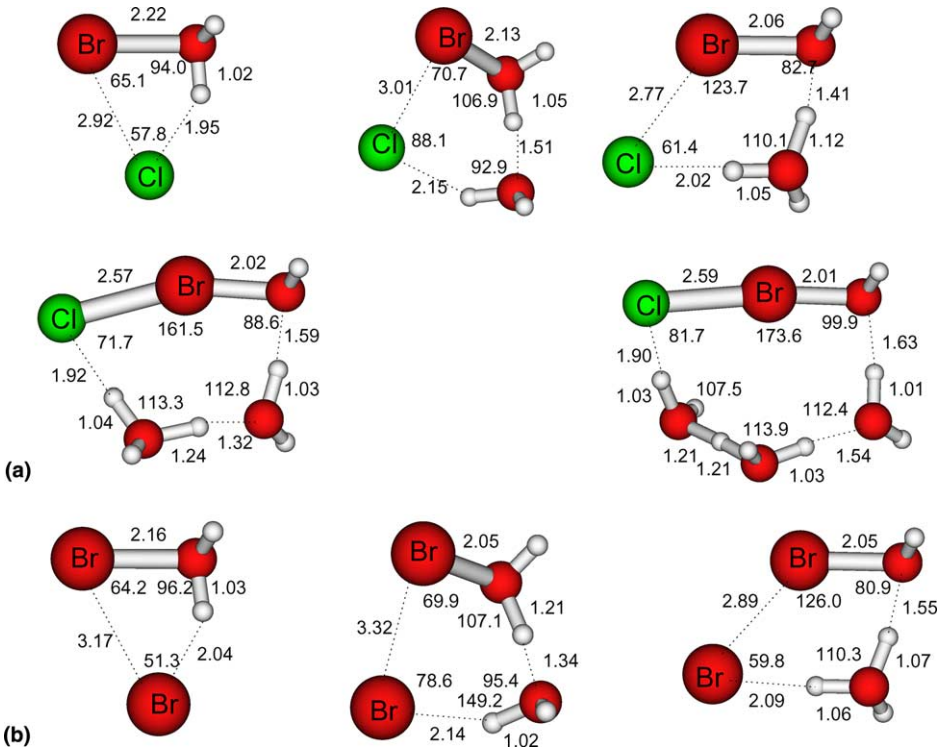

Fig. 2. Structures of the transition states of the different mechanisms. (a) shows the transition states of the reactions HOBr + HCl + nH$_2$O ($n = 0$, 1, 2 and 3), whereas (b) shows the transition states for the reactions of HOBr + HBr + nH$_2$O ($n = 0$ and 1) according to the mechanisms as introduced in Fig. 1. (Units are in Å and degrees.)

Table 1
Reaction barriers for the reactions HOBr + HCl and HOBr + HBr catalyzed by n water molecules at different levels of theory

	B3LYP		MPW1K
	6-31+G(d)	6-311++G(d,p)	6-31+G(d,p)
HOBr + HCl			
$n = 0$	32.3	32.2	41.6
$n = 1$a	33.4	32.8	42.1
$n = 1$b	26.1	27.9	33.1
$n = 2$	2.57	3.87	2.88
$n = 3$	0.349	0.421	0.095
HOBr + HBr			
$n = 0$	23.1	23.4	31.1
$n = 1$a	25.6	24.3	32.2
$n = 1$b	20.4	19.7	20.3

3.1.1. HOBr + HCl

The reaction complex (RC) is characterized by a hydrogen bond between the HCl hydrogen and the HOBr oxygen. The proton is transfered along the hydrogen bond forming a proton-shifted $HOH^+Br \cdot Cl^-$ complex at the transition state (see Fig. 2). Then the bromine moiety is released and comes in contact with the chlorine forming a BrCl molecule. The reaction barrier is 41.6 kcal mol^{-1} (see Table 1 for reaction barriers and Table 2 for reaction energies) which is remarkably 13.1 kcal mol^{-1} lower than the reaction barrier of the analogous reaction HOCl + HCl [11].

3.1.2. HOBr + HCl + 1H$_2$O

Two different local minimum structures for the $HOBr \cdot HCl \cdot H_2O$ complex termed (1a) and (1b) (see Fig. 1) were characterized. Reaction complex (1a) is a lower lying local minimum compared to (1b) differing by 1.11 kcal mol^{-1}. At 200 K, which is a stratospherically relevant temperature, (1a) would be approximately 16 times more populated. Mechanistically, in both reaction channels complexes are formed where the water molecule is

Table 2
Reaction energies for the reactions HOBr + HCl and HOBr + HBr catalyzed by n water molecules at different levels of theory

	B3LYP		MPW1K
	6-31+G(d)	6-311++G(d,p)	6-31+G(d,p)
HOBr + HCl			
$n = 0$	−19.1	−19.4	−20.3
$n = 1a$	−18.2	−18.9	−18.9
$n = 1b$	−20.3	−20.0	−19.9
$n = 2$	−21.6	−21.0	−22.0
$n = 3$	−18.4	−19.3	−18.5
HOBr + HBr			
$n = 0$	−30.3	−29.9	−31.4[a]
$n = 1a$	−27.8	−29.1	−29.5
$n = 1b$	−27.9	−30.2	−33.1

[a] Energy calculated with MPW1K/6-31+G(d,p) using the geometries obtained at the B3LYP/6-311++G(d,p) level of theory [shorthand notation: MPW1K/6-31+G(d,p)//B3LYP/6-311++G(d,p)].

inserted between HCl and HOBr. HCl is a hydrogen bond donor, HOBr is again the hydrogen bond acceptor at the oxygen position, whereas the water molecule is both hydrogen bond acceptor (for HCl) and hydrogen bond donor (for HOBr). The reaction proceeds via 'water-mediated proton transfer' using the water molecule as proton shuttle. In such water assisted proton transfer mechanisms, the water molecule very often has a strong catalytic effect [11,33]. However, the reaction barrier of reaction channel (1b) is 33.1 kcal mol^{-1} whereas for channel (1a) it is 42.1 kcal mol^{-1} making reaction channel (1b) much more likely even though it starts from an energetically slightly disfavored minimum. Yet, the barrier of reaction channel (1a) is almost identical to the water-free reaction. Therefore, this mechanism is more or less unimportant since it does not provide any energetic advantage compared to the water free reaction. In comparison to the HOCl reactions, mechanism (1a) has a 12.6 kcal mol^{-1} lower barrier, yet mechanism (1b) has exactly the same barrier at the MPW1K/6-31+G(d,p) level of theory and also at the B3LYP/6-31+G(d) level [11].

3.1.3. $HOBr + HCl + 2H_2O$

The mechanism of this reaction is similar to the above mentioned ones. Yet, instead of a single water molecule the mechanism now involves a water dimer, since the second water molecule in the RC is also located between HCl and HOBr and it participates actively in the reaction. Water molecule number 2 is both proton donor and acceptor, thus, both water molecules 'shuttle' a proton of the hydrogen bond donor HCl to the oxygen of the hydrogen bond acceptor HOBr. The catalytic influence of the two water molecules is remarkable. The barrier is reduced to only 2.88 kcal mol^{-1} which is 30 kcal mol^{-1} lower than in mechanism (1b). The analogous HOCl reaction has a barrier of 9.74 kcal mol^{-1} [11] which is almost 7 kcal mol^{-1} higher than the reaction with HOBr.

3.1.4. $HOBr + HCl + 3H_2O$

Finally, we investigated the reaction of HOBr with HCl involving three water molecules. As outlined in Fig. 1 the mechanism is similar as for the reaction with two water molecules now involving a water trimer. In the RC, HCl has already protonated the first neighboring water molecule forming a $H_3O^+ \cdot Cl^-$ complex. The following steps are in analogy as before—the hydronium ion protonates the second water molecule, which protonates the third water molecule which finally protonates HOBr. The third water molecule has an additional catalytic effect since this reaction can be considered to be almost barrierless because the reaction barrier is only 0.1 kcal mol^{-1}. (By calculation of the MEP we could confirm that the identified transition state is connected with the determined reactant and product.) This is 3 kcal mol^{-1} lower than the reaction of HOCl [11]. Considering the structure of the RC, the orientation of the water molecules is almost as it is on a hexagonal ice surface. Thus, on ice-like PSCs the reaction of HOBr with an adsorbed HCl molecule should not be hindered by any reaction barrier.

3.1.5. $HOBr + HBr + nH_2O$

Qualitatively the reactions of HOBr with HBr are equivalent to the reactions involving HCl, at least for the reactions with 0 and with 1 water molecule. For the gas-phase reaction HOBr + HBr the barrier is 31.1 kcal mol^{-1} which is 10.5 kcal mol^{-1} lower than the HCl reaction and 13.3 kcal

mol^{-1} lower than the HOCl + HBr reaction [11]. For the reactions with one catalytic water molecule, the same mechanisms as mentioned above have been found and the barriers are 32.2 and 20.3 kcal mol^{-1}, respectively. Again, in mechanism (1a) the water molecule has no catalytic effect, whereas in mechanism (1b) the barrier is reduced by 10.8 kcal mol^{-1} in comparison to the uncatalyzed reaction. The preassociation complexes are similar in energy differing by less than 0.1 kcal mol^{-1}, so both minima are almost equally populated. However, the reactions with more than one water molecule could not be characterized, since they seem to be barrierless at the levels of theory that we employed. We were unable to characterize transition states and the reaction complexes for these systems. Compared to the HCl reaction but most of all compared to the HOCl + HBr reactions, this observation is not unexpected. The reaction of HOCl + HBr + $2H_2O$ has a barrier of 0.76 kcal mol^{-1} and the reaction of HOCl + HBr + $3H_2O$ has a barrier of 0.75 kcal mol^{-1} [11]. Considering that in all cases substitution of chlorine atoms by bromine atoms lowered the reaction barrier, the reaction of HOBr + HBr with two or more catalytic water molecules can be expected to be barrierless.

3.2. Reaction rates and quantum mechanical tunneling

Accurate calculations of rate constants for reactions involving hydrogen atom transfer require a quantum mechanical treatment of the motion along the reaction coordinate. This in turn requires knowledge of the PES beyond the stationary points. In proton transfer reactions, tunneling very often increases the reaction rate constant by many orders of magnitude [34,35].

Fig. 3 shows unimolecular reaction rates in the series HOBr + HCl supported by $n = 0$, 1, and 2 water molecules and HOBr + HBr supported by $n = 0$ and 1 water molecules. No reaction rates were determined for the reaction HOBr + HCl + $3H_2O$ since the barrier is only 0.1 kcal mol^{-1}. In this case we are close to the diffusional limit that is why we did not calculate reaction rate constants by VTST. As expected from the reaction barriers the

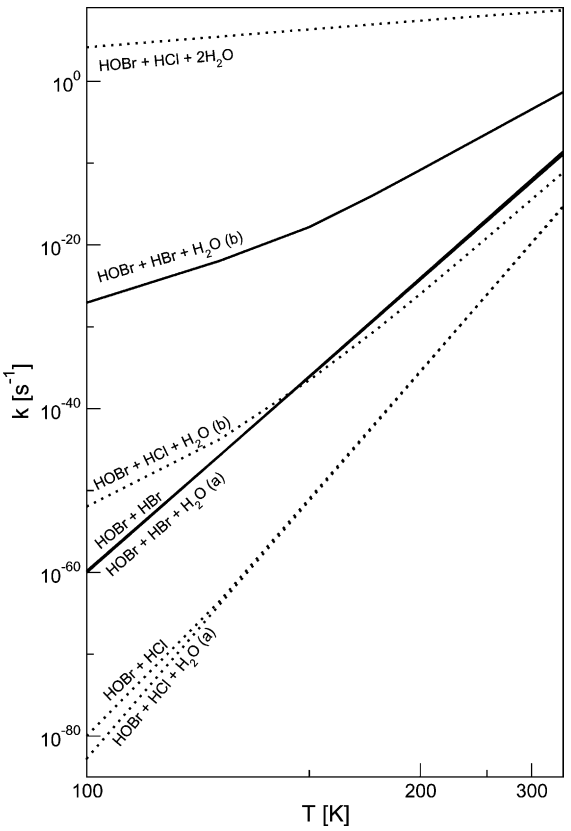

Fig. 3. Reaction rates for the reactions of HOBr with HCl (dotted line) and HBr (full line). The reactions HOBr + HBr and HOBr + HBr + $1H_2O$ (a) are almost equally fast as are the reactions HOBr + HCl and HOBr + HCl + $1H_2O$ (a). The reaction HOBr + HCl + $2H_2O$ is the fastest reaction shown. Reactions of HOBr + HCl with >2 water molecules and reactions of HOBr + HBr with $\geqslant 2$ water molecules are barrierless and therefore not shown.

reactions involving HBr are generally faster than the reactions involving HCl. The reaction rate for the reaction HOBr + HCl with 2 water molecules is only slightly temperature dependent. This is reflected in the small change of the reaction rate constant in the interval 190–300 K of a factor of 15.

The transmission coefficients for quantum mechanical tunneling along the reaction coordinate are summarized in Table 3 for 190 K. In general, the small-curvature tunneling approach is predominant over LCT. The highest tunneling contributions were found for the reactions HOBr

Table 3
Transmission coefficients κ determined by small and LCT for the HOBr + HCl, HBr reactions at 190 K

	Transmission coefficient κ at 190 K	
	LCT	SCT
HOBr + HCl		
$n = 0$	1.47	**1.49**
$n = 1a$	1.13	**1.21**
$n = 1b$	5.86	**6.67**
$n = 2$	1.27	**1.36**
HOBr + HBr		
$n = 0$	1.31	**1.35**
$n = 1a$	1.21	**1.30**
$n = 1b$	1.72	**2.00**

SCT is the predominant form of tunneling as highlighted in bold.

+ HCl + $1H_2O$ (1b) and HOBr + HBr + $1H_2O$ (1b) with κ values of 6.67 and 2.00, respectively. Thus, tunneling enhances the reaction rates by 567% and 100%, respectively. The higher tunneling contribution for mechanisms (1b) in comparison to (1a) might be best explained by inspecting Fig. 4. The barrier of channels (1b) is much narrower than for the channels (1a). Detailed inspection of the mechanism showed that the mechanisms of (1a) work as follows: First, the proton of HOBr flips approximately 120° along the Br–O bond. Then, the bromine and chlorine (or bromine) atoms move approximately 1.24 Å (for HOBr + HCl) or 1.40 Å (for HOBr + HBr) towards each other at the transition state.

Comparison of the gas-phase reaction HOBr + HCl with the reaction involving $n = 2$ water molecules reveals that the reaction rate enhancement is 50 orders of magnitude at 190 K. To illustrate this huge difference, the gas-phase reaction happens within 2.4×10^{30} years, whereas the catalyzed reaction happens within picoseconds.

4. Conclusions

In this study we have investigated the competing reactions of HOBr + HCl and HOBr + HBr either in the gas phase or on model water clusters representative of hexagonal ice. Reaction rates were determined using VTST including tunneling

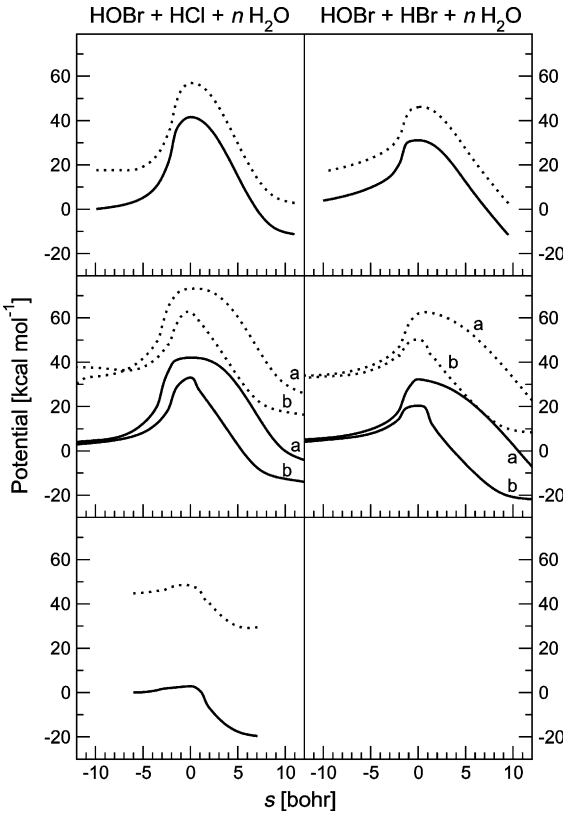

Fig. 4. Classical potential energy curve (or potential along the MEP; full line), and vibrationally adiabatic ground-state potential energy curve (dotted line) as a function of the reaction coordinate s calculated at the B3LYP/6-31+G(d) level of theory interpolated to MPW1K/6-31+G(d,p) energies. Left: HOBr + HCl + nH$_2$O starting from $n = 0$ (top) down to $n = 2$ (bottom); right: HOBr + HBr + nH$_2$O ($n = 0$ and 1).

corrections. A trend of increasing reaction rate constants by including catalytic water molecules in the reaction could be observed. The uncatalyzed HOBr + HCl reaction is 50 orders of magnitude slower than the reaction occurring on a water cluster composed of only two water molecules. Reactions of HOBr + HBr are even barrierless in the presence of two or more water molecules, making these reactions very fast. The contribution of tunneling enlarges the reaction rate constants at 190 K between 21% and 567%. A direct comparison of the analogous HCl and HBr reactions reflects that the HBr reactions with HOBr are in general faster. A comparison with the analogous reactions of HOCl with HX (X = Cl, Br) shows

that reactions including more bromine atoms are faster than reactions with chlorine. The reactions of HOCl + HBr and HOBr + HCl proceed at similar rates. Thus, considering polar stratospheric conditions, the reactions of HOBr with HBr are the most reactive ones.

Acknowledgements

This study was supported by the Austrian Science Fund (project number P14357-TPH).

References

[1] S. Solomon, Rev. Geophys. 37 (1999) 275.
[2] B.J. Finlayson-Pitts, J.N. Pitts Jr., Chemistry of the Upper and Lower Atmosphere, Academic Press, San Diego, London, 2000.
[3] M.J. Molina, T.-L. Tso, L.T. Molina, F.C.-Y. Wang, Science 238 (1987) 1253.
[4] D.J. Lary, M.P. Chipperfield, R. Toumi, T. Lenton, J. Geophys. Res. 101 (1996) 1489.
[5] M.J. Prather, Nature 255 (1992) 534.
[6] L. Chu, L.T. Chu, J. Phys. Chem. A 103 (1999) 691.
[7] S.L. Richardson, J.S. Francisco, A.M. Mebel, K. Morokuma, Chem. Phys. Lett. 270 (1997) 395.
[8] Z.F. Liu, C.K. Siu, J.S. Tse, Chem. Phys. Lett. 309 (1999) 335.
[9] S.C. Xu, J. Chem. Phys. 111 (1999) 2242.
[10] Y.-F. Zhou, C.-B. Liu, Int. J. Quant. Chem. 78 (2000) 281.
[11] A.F. Voegele, C.S. Tautermann, T. Loerting, K.R. Liedl, J. Phys. Chem. A 106 (2002) 7850.
[12] S. Solomon, M. Mills, L.E. Heidt, W.H. Pollock, A.F. Tuck, J. Geophys. Res. 97 (1992) 825.
[13] C.T. McElroy, C.A. McLinden, J.C. McConnell, Nature 397 (1999) 338.
[14] K.L. Foster, R.A. Pastridge, J.W. Bottenheim, P.B. Shepson, B.J. Finlayson-Pitts, C.W. Spicer, Science 291 (2001) 471.
[15] G.C.G. Waschewsky, J.P.D. Abbatt, J. Phys. Chem. A 103 (1999) 5312.
[16] L. Chaix, A. Allanic, M.J. Rossi, J. Phys. Chem. A 104 (2000) 7268.
[17] B.A. Flowers, J.S. Francisco, J. Phys. Chem. A 105 (2001) 494.
[18] P.J. Stephens, F.J. Devlin, C.F. Chabalowski, M.J. Frisch, J. Phys. Chem. 45 (1994) 11623.
[19] B.J. Lynch, P.L. Fast, M. Harris, D.G. Truhlar, J. Phys. Chem. A 104 (2000) 4811.
[20] M.J. Frisch et al., Gaussian98, Revision A.9, Gaussian, Inc., Pittsburgh, PA, 1998.
[21] M. Page, J.W. McIver Jr., J. Chem. Phys. 88 (1988) 922.
[22] J.L. Durant, Chem. Phys. Lett. 256 (1996) 598.
[23] Y.-Y. Chuang, D.G. Truhlar, J. Phys. Chem. A 101 (1997) 3808.
[24] J.C. Corchado et al., Polyrate9.0, University of Minnesota, Minneapolis, 2002.
[25] J.C. Corchado et al., Gaussrate9.0, University of Minnesota, Minneapolis, 2002.
[26] D.G. Truhlar, B.C. Garrett, Ann. Rev. Phys. Chem. 35 (1984) 159.
[27] D.G. Truhlar, A.D. Isaacson, B.C. Garrett, Generalized Transition State Theory, CRC Press, Boca Raton, FL, 1985, p. 65.
[28] M.M. Kreevoy, D.G. Truhlar, Transition State Theory, John Wiley & Sons, Inc., New York, 1986, p. 13.
[29] S.C. Tucker, D.G. Truhlar, Dynamical Formulation of Transition State Theory: Variational Transition States and Semiclassical Tunneling, NATO ASI Series C, vol. 267, Kluwer, Dordrecht, The Netherlands, 1989, p. 291.
[30] D.G. Truhlar, Direct Dynamics Method for the Calculation of Reaction Rates, Kluwer, Dordrecht, 1995, p. 229.
[31] Y.-P. Liu, G.C. Lynch, T.N. Truong, D.-h. Lu, D.G. Truhlar, B.C. Garrett, J. Am. Chem. Soc. 115 (1993) 2408.
[32] A. Fernández-Ramos, D.G. Truhlar, J. Chem. Phys. 114 (2001) 1491.
[33] T. Loerting, K.R. Liedl, J. Phys. Chem. A 105 (2001) 5137.
[34] T. Loerting, K.R. Liedl, B.M. Rode, J. Am. Chem. Soc. 120 (1998) 404.
[35] T. Loerting, K.R. Liedl, B.M. Rode, J. Chem. Phys. 109 (1998) 2672.